

Intrinsic regulation of muscle contraction

François Kimmig, M Caruel, D Chapelle

► **To cite this version:**

François Kimmig, M Caruel, D Chapelle. Intrinsic regulation of muscle contraction. VPH 2020 - Virtual Physiological Human, Aug 2020, Paris, France. hal-03156494

HAL Id: hal-03156494

<https://hal-cnrs.archives-ouvertes.fr/hal-03156494>

Submitted on 2 Mar 2021

HAL is a multi-disciplinary open access archive for the deposit and dissemination of scientific research documents, whether they are published or not. The documents may come from teaching and research institutions in France or abroad, or from public or private research centers.

L'archive ouverte pluridisciplinaire **HAL**, est destinée au dépôt et à la diffusion de documents scientifiques de niveau recherche, publiés ou non, émanant des établissements d'enseignement et de recherche français ou étrangers, des laboratoires publics ou privés.

Intrinsic regulation of muscle contraction

F. Kimmig^{a,c,*}, M. Caruel^b, D. Chapelle^{c,a}

^aLMS, CNRS, École polytechnique, Institut Polytechnique de Paris, France

^bMSME, CNRS, Université Paris-Est, France, ^cInria, France

Keywords muscle modelling, contraction regulation, length-dependence effects

1. Introduction

In the context of cardiac muscle modelling, the active force developed through the interaction between myosin heads and actin sites is regulated at the microscopic level resulting at the organ level into adaptation capabilities, including the Frank-Starling mechanism. This regulation is of two kinds: (i) intrinsic as a result of the sarcomere stretch and (ii) extrinsic through the neuroendocrine regulation. In this work, we focus on the intrinsic regulation, which come from from a variation of the number of available myosin heads and the number of activated actin sites as a result of the stretch of the sarcomere level [4] but leaves the individual actin-myosin mechanical interaction unchanged [2, 10]. We say that the myosin and actin filaments have a varying activation level.

We propose here a new approach that allows to incorporate these two variations into the classical Huxley'57 muscle contraction model equations [7]. This approach allows to bridge the numerous work that have been conducted, on the modelling of the actin-myosin interaction on the one side [6, 9, 1, 3], and the modelling of the thin filament activation on the other side [11, 13], into a complete modelling framework.

2. Model presentation

2.1 Myosin filament activation

The original Huxley'57 model describes the myosin head by two states: attached and detached and assumes that all myosin heads and all actin sites are activated. The varying availability of the myosin heads is introduced by considering two pools of heads: heads that are available for attachment and heads that are not. The heads that are not available can still attach but with a much slower rate. The fraction available heads is given by n_0 and is assumed to depend only on the sarcomere extension e_c . In each pool, the probability of being attached for a group of myosin heads located at distance s from their nearest actin site is denoted by $P_1(s, t, \gamma)$, where the additional discrete variable γ describes the belonging to one of the two pools. The variable γ takes the value 1 in the pool of the available heads and takes the value 0 in the other pool. In each pool, the myosin head can transition between the two possible states with the attachment rate f_γ and detachment rates g_γ . Defining $|x|_+$ by x , if $x \geq 0$

and zero otherwise and $|x|_- = -x + |x|_+$, the dynamics of the system is given by

$$\left\{ \begin{array}{l} \frac{d}{dt} P_1(s, t, 1) = \partial_t P_1(s, t, 1) + \dot{x}_c \partial_s P_1(s, t, 1) \\ \quad + \frac{|\dot{n}_0|_+}{n_0} [P_1(s, t, 1) - P_1(s, t, 0)] = \\ \quad f_1(s)(1 - P_1(s, t, 1)) - g_1(s)P_1(s, t, 1), \\ \frac{d}{dt} P_1(s, t, 0) = \partial_t P_1(s, t, 0) + \dot{x}_c \partial_s P_1(s, t, 0) \\ \quad + \frac{|\dot{n}_0|_-}{1 - n_0} [P_1(s, t, 0) - P_1(s, t, 1)] = \\ \quad f_0(s)(1 - P_1(s, t, 0)) - g_0(s)P_1(s, t, 0), \end{array} \right.$$

where \dot{x}_c is the relative sliding velocity between the myosin and actin filaments.

2.2 Actin filament activation

We now extend this model to rigorously incorporate the variation of the thin filament activation. We supplement our myosin head model with the actin site activation kinetics, which will be characterised by a new parameter n_a , denoting the ratio of activated actin sites. An actin site exists in four possible states: (i) non activated and non occupied by a myosin head, (ii) activated and non occupied, (iii) non activated but occupied a myosin head or (iv) activated and occupied. We establish, in each pool of myosin heads, the governing system of equations with conservation laws. The system can be reduced to

$$\left\{ \begin{array}{l} \frac{d}{dt} P_1(s, t, \gamma) = f_{\gamma,a}(s) \bar{n}_a(s, t, \gamma) \\ \quad + f_{\gamma,na}(s)(1 - P_1(s, t, \gamma) - \bar{n}_a(s, t, \gamma)) \\ \quad - g_{\gamma,a}(s)(n_a - \bar{n}_a(s, t, \gamma)) \\ \quad - g_{\gamma,na}(s)(\bar{n}_a(s, t, \gamma) - n_a + P_1(s, t, \gamma)), \\ \frac{d}{dt} \bar{n}_a(s, t, \gamma) = \frac{|\dot{n}_a|_+}{1 - n_a} (1 - P_1(s, t, \gamma) - \bar{n}_a(s, t, \gamma)) \\ \quad + g_{\gamma,a}(s)(n_a - \bar{n}_a(s, t, \gamma)) \\ \quad - \frac{|\dot{n}_a|_-}{n_a} \bar{n}_a(s, t, \gamma) - f_{\gamma,a}(s) \bar{n}_a(s, t, \gamma), \end{array} \right.$$

where \bar{n}_a denotes the ratio of actin sites that are activated but non-occupied. The active tension is given by the average between the two pools of myosin heads.

3. Validation

We validate our model by comparing its outputs with experimental data. The model is calibrated

*Corresponding author. Email: francois.kimmig@inria.fr

choosing n_0 such that the predicted tension interpolates data points in maximal calcium activation conditions. The input parameter n_a is written as $n_a = n_{a,\infty}(e_c, C)n_{a,t}(e_c, t)$. The function $n_{a,\infty}(e_c, C)$, where $C \in [0, 1]$ denotes a normalised level of calcium activation, accounts for the steady-state activation and is chosen as a sigmoid function to mimic the experimental data obtained on skinned cells [5]. The function $n_{a,t}(e_c, t)$ captures the transient nature of the thin filament activation.

We first compare the steady-state model prediction with experimental data obtained in [12] (see Figure 1) and note that our model displays a good match with the data. We then compare the dynamics predicted by the model with data from [8]. We simulate twitch contractions in “high” and “low” contractility conditions (corresponding to a “high” and “low” level of calcium supply, respectively) in isometric conditions, i.e. with $\dot{x}_c = 0$ (see Figure 2). The results match well the experimental data in high contractility conditions. However, in low contractility conditions, the decreases of the peak force with the sarcomere extension is faster in the simulations than in the data. One can note that this decrease originates from the constraints imposed on the function $n_{a,\infty}$ by the steady-state data. However, these data are obtained on a range of sarcomere extensions where the function $n_{a,\infty}$ extrapolates the data.

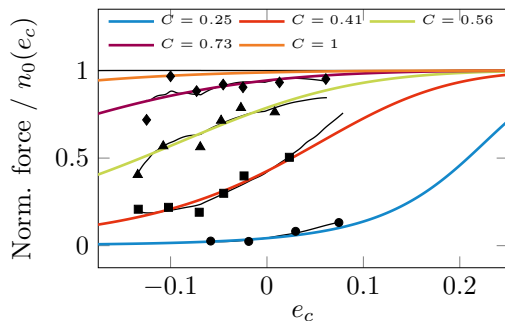


Figure 1: Steady state thin filament activation. Experimental data (black closed symbols) and model outputs (coloured lines).

4. Conclusion

In this work, we proposed a novel framework to rigorously incorporate the varying myosin heads and actin sites activation level into the Huxley’57 model family. This framework may be coupled to a separately defined thin filament activation model or, as done in this work, used as a standalone model with the time-dependent thin filament activation being provided as a model input. The model is calibrated on experimental twitch contractions obtained in controlled sarcomere length conditions and a preliminary validation is performed.

5. References

[1] M. Caremani et al. *J Physiol*, 593(15):3313–3332, July 2015.

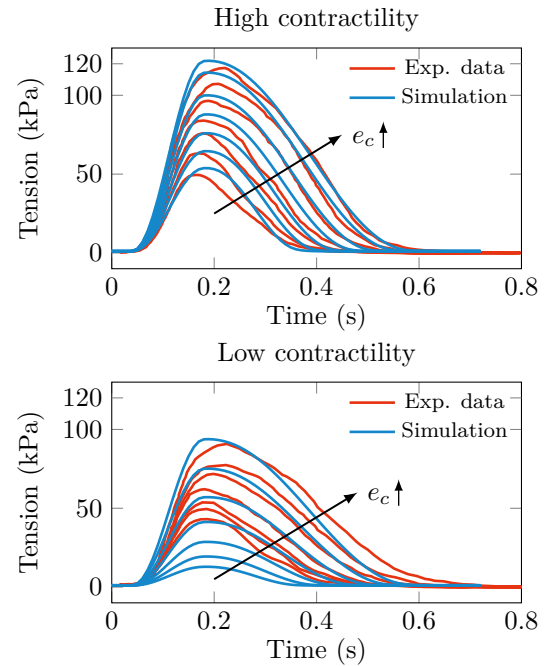


Figure 2: Transient twitch contraction at various sarcomere stretch in sarcomere length control conditions. Experimental data (red lines) and model outputs (blue lines). The sarcomere extension e_c varies between 0.027 and 0.189.

- [2] M. Caremani et al. *PNAS USA*, 113(13):3675–3680, March 2016.
- [3] M. Caruel et al. *Biomech Model Mechanobiol*, 18(3):563–587, 2019.
- [4] P.P. de Tombe et al. *J Mol Cell Cardiol*, 48(5):851–858, May 2010.
- [5] D.P. Dobesh et al. *Am J Physiol Heart Circ Physiol*, 282(3):H1055–H1062, March 2002.
- [6] E. Eisenberg et al. *Biophys J*, 29(2):195–227, February 1980.
- [7] A.F. Huxley. *Progr Biophys Chem*, 1957.
- [8] P.M. Janssen et al. *Am J Physiol Heart Circ Physiol*, 269(2):H676–H685, August 1995.
- [9] L. Marcucci et al. *Phys Rev E*, 81(5):051915–8, May 2010.
- [10] F. Pinzauti et al. *J Physiol*, 596(13):2581–2596, May 2018.
- [11] J.J. Rice et al. *Biophys J*, 84(2):897–909, February 2003.
- [12] H.E.D.J. ter Keurs et al. *Prog Biophys Mol Bio*, 97(2-3):312–331, June 2008.
- [13] T. Washio et al. *Cell Mol Bioeng*, 5(1):113–126, December 2011.